

On the simulation of nonlinear bidimensional spiking neuron models

Jonathan Touboul

NeuroMathComp Laboratory, INRIA/ENS Paris, Paris, France

May 25, 2022

Abstract

Bidimensional spiking models currently gather a lot of attention for their simplicity and their ability to reproduce various spiking patterns of cortical neurons, and are particularly used for large network simulations. These models describe the dynamics of the membrane potential by a nonlinear differential equation that blows up in finite time, coupled to a second equation for adaptation. Spikes are emitted when the membrane potential blows up or reaches a threshold value θ . The precise simulation of the spike times and of the adaptation variable is critical for it governs the spike pattern produced, and is hard to compute accurately because of the diverging nature of the system at the spike times. We precisely study fixed time-step integration scheme for this time of models and demonstrate that these methods produce systematic errors that are unbounded as the threshold increases in both the evaluation of the two crucial values: the value of the spike time and the value of the adaptation variable at this time, and precise evaluation of these involve very small time steps and therefore long simulation times. In order to achieve a fixed predetermined precision in a reasonable computational time, we propose here a new algorithm to simulate these system based on a variable integration step method that either integrates the original ordinary differential equation or the equation of the orbits in the phase plane, and compare the two algorithms in numerical simulations.

1 Introduction

The biophysics of neurons and their ionic channels are now understood in great details, although many questions still remain open [8]. This better understanding allows to propose very precise models of neurons mimicking the dynamics

of ionic transfers through the channels. Yet, simple neuron models such as the integrate-and-fire model [16, 6] remain very popular in the computational neuroscience community, because they can be simulated very efficiently and, perhaps more importantly, because they are easier to understand and analyze. The drawback is that these simple models cannot account for the variety of electrophysiological behaviors of real neurons (see e.g. [18] for interneurons). Recently, several authors introduced two-variable spiking models [11, 2, 24] which, despite their simplicity, can reproduce a large number of electrophysiological signatures such as bursting or regular spiking. Different sets of parameter values correspond to different electrophysiological classes.

These models seem to provide a compromise between simplicity and versatility. Simplicity, in the sense that it allows analytical studies [24, 27], efficient numerical simulations for very large networks simulations [13], and few parameters that can be precisely fitted to intracellular recordings [3, 14, 15]. And versatility, because it is able to reproduce a variety of possible behaviors that neurons present: in [11, 24], the authors provide simulations corresponding to a wide variety of neuronal behaviors, and simple sets of parameters corresponding to each behaviors can be determined, either analytically [24, 27] or numerically [19], and that can be precisely tuned to fit intracellular recordings. These models also aroused the interest of mathematicians, for the nonlinear nature of the dynamics combined with the discrete nature of spikes makes of this class of models an interesting novel mathematical object [24, 27].

These models describe the dynamics of the membrane potential by a nonlinear differential equation, coupled to a second equation for adaptation, and a separate discrete mechanism accounts for the spike emission. In details, these models satisfy reduced equations of the type:

$$\begin{cases} \frac{dv}{dt} &= F(v) - w + I \\ \frac{dw}{dt} &= a(bv - w) \end{cases} \quad (1)$$

where a and b are non-negative parameters accounting respectively for the time scale of the adaptation variable with respect to the membrane potential's time scale and for the coupling strength between the two variables. The function $F(\cdot)$ is a real function, that satisfies the following assumptions:

Assumption (A1).

1. F is regular (at least three times continuously differentiable)
2. F is strictly convex, and $\lim_{x \rightarrow -\infty} F'(x) \leq 0$,
3. There exists $\varepsilon > 0$ and $\alpha > 0$ for which $F(v) \geq \alpha v^{1+\varepsilon}$ when $v \rightarrow \infty$ (we will say that F grows faster than $v^{1+\varepsilon}$ when $v \rightarrow \infty$).

Under these assumptions, the membrane potential blows up in finite time for some initial conditions (see [27] and section 4). A spike is emitted at the time t^* when the membrane potential v reaches a cutoff value θ or when it blows

up. At this time, the membrane potential is reset to a constant value c and the adaptation variable is updated to $w(t^*) + d$ where $w(t^*)$ is the value of the adaptation variable at the time of the spike and $d > 0$ is the spike-triggered adaptation parameter. Furthermore, if the function F satisfies the assumption:

Assumption (A2). *There exists $\varepsilon > 0$ and $\alpha > 0$ for which $F(v) \geq \alpha v^{2+\varepsilon}$ when $v \rightarrow \infty$ (F grows faster than $v^{2+\varepsilon}$ when $v \rightarrow \infty$),*

then the adaptation variables converges to a finite value when the membrane potential blows up, which allows replacement of the strict voltage threshold of classical (linear) integrate-and-fire neurons [16, 21] by a more realistic smooth spike initiation (see e.g. [17, 5]).

Among these models, the widely used *quadratic adaptive* model [11] corresponds to the case where $F(v) = v^2$, and has been recently used by Eugene Izhikevich and coworkers [13] in very large scale simulations of neural networks. This model does not satisfies assumption (A2), and in that case the adaptation variable w blows up at the times of the spikes, which implies that the spike patterns produced by the simulation of this model sensitively depends on the choice of the cutoff, parameter which does not have any biological interpretation (see [25]). The *adaptive exponential* model [2] corresponds to the case where $F(v) = e^v - v$. It has the interest that its parameters can be related to electrophysiological quantities, and has been successfully fit to intracellular recordings of pyramidal cells [3, 14, 1]. The *quartic* model [23] corresponds to the case where $F(v) = v^4 + \alpha v$. It has the advantage of being able to reproduce all the behaviors featured by the other two and also self-sustained subthreshold oscillations which are of particular interest to model certain nerve cells.

In these models, the neural code is assumed to be contained in the times of the spikes. Therefore, computing the spike times with accuracy is essential. Moreover, the reset mechanism makes critical the value of the adaptation variable at the time of the spike. Indeed, when a spike is emitted at time t^* , the new initial condition of the system (1) is $(c, w(t^*) + d)$. Therefore, this value $w(t^*)$ governs the subsequent evolution of the membrane potential, and hence the spike pattern produced. For instance in [26, 25, 27], the authors show that the sequence of reset locations after each spike time shapes the spiking signature of the neuron. They also show that small perturbations can result in dramatic changes, since the spike pattern produced presents bifurcations.

The explosion of the membrane potential variable (and possibly of the adaptation variable) makes the simulation of these models very delicate. Indeed, the explosion implies that the membrane potential v , as a function of time, presents singularities at the spike times, where in particular both the membrane potential and the adaptation variables have an infinite derivative (the explosion in finite time always corresponds to an infinite derivative, and equation (1) implies that at these times the derivative of w also tends to infinity¹). This property of the model makes the accurate simulation of these models very difficult. For

¹it can be easily proved that when $w(t)$ is always dominated by $v(t)$ (i.e. $w = o(v(t))$) at the explosion times

mono-dimensional models where no adaptation (variable w) is taken into account, the spike time can be corrected following [5] by computing the explosion time in close form, which allows a good evaluation of the spike times. This approach is not possible for bidimensional models including adaptation, that are nevertheless more realistic from a biological viewpoint.

In this paper, we start by proving in section 2 some theoretical results on the model that characterize the trajectories of the solutions of the equations (1) in the phase plane and that will be useful for our applications. We next thoroughly study in section 3 the precision of fixed time step methods such as the Euler integration scheme that are the most widely used methods to simulate such equations. We will observe that the error made is unbounded as the threshold θ increases, which lead us to propose in section 4 a new algorithm for accurately and efficiently simulating the solutions of these equations, and in particular two crucial features of the model, namely the spike time and the value of the adaptation variable at these times.

2 Some Theoretical Results

We recall that the dynamical system (1), governed by a two dimensional vector field, can present zero, one or two fixed points depending on the values of the parameters. More precisely, let us denote by $m(b)$ the unique minimum of the convex function $v \mapsto F(v) - bv$, and by $v^*(b)$ the unique point where this minimum is reached (i.e. the unique solution of $F'(v^*(b)) = b$, which exists under assumption (A1)). It is prove in [24] (see figure 1) that:

- if $I > -m(b)$ then the system has no fixed point;
- if $I = -m(b)$ then the system has a unique fixed point, $(v^*(b), w^*(b))$, which is non-hyperbolic. It is unstable if $b > a$.
- if $I < -m(b)$ then the dynamical system has two fixed points $(v_-(I, b), v_+(I, b))$ such that

$$v_-(I, b) < v^*(b) < v_+(I, b).$$

The fixed point $v_+(I, b)$ is a saddle fixed point, and the stability of the fixed point $v_-(I, b)$ depends on I and on the sign of $(b - a)$:

1. If $b < a$ then the fixed point $v_-(I, b)$ is attractive.
2. If $b > a$, there is a unique smooth curve $I^*(a, b)$ defined by the implicit equation $F'(v_-(I^*(a, b), b)) = a$. This curve reads $I^*(a, b) = bv^*(a) - F(v^*(a))$ where $v^*(a)$ is the unique solution of $F'(v^*(a)) = a$.
 - (a) If $I < I^*(a, b)$ the fixed point is attractive.
 - (b) If $I > I^*(a, b)$ the fixed point is repulsive.

In [27], the authors thoroughly define a Markov partition of the dynamics in each case, that involve a *spiking zone* which is stable under the flow and where any orbit with initial condition in the zone blows up in finite time (and fires a

spike). The precise description of this zone is quite complex and involves the description of the stable manifold of the saddle fixed point $v_+(I, b)$, which does not have a simple analytical expression. We are interested here in defining a subzone of the spiking zone stable under the flow of the differential equation that allows a simple computation of the spike time and of the adaptation variable at this time, and turn to the definition of a special zone in the parameter through the following definition:

Definition 1. Let $Z(V)$ be the zone in the phase plane (v, w) defined as:

$$Z(V) = \{(v, w) \in \mathbb{R}^2 ; v > V \text{ and } w < bv\}.$$

Note that $Z(V)$ constitute a decreasing family of nested sets. We further define, when the input current I is constant,

$$Z(I, b) = \cup_{V > v_+(I, b)} Z(V),$$

where $v_+(I, b)$ is the larger fixed point of the system (1) when it exists, and $-\infty$ if it does not. We have:

- If $I > -m(b)$, then $Z(I, b) = \{(v, w) \in \mathbb{R}^2 ; w < bv\}$.
- If $I < -m(b)$, then $Z(I, b) = \{(v, w) \in \mathbb{R}^2 ; v > v_+(I, b) \text{ and } w < bv\}$

These subsets of the phase plane present the interest to satisfy the following properties

Theorem 1. *Assume that the input current $I(t)$ depends on time, and moreover that $t \mapsto I(t)$ is lower bounded (at least on the time interval considered (τ_0, τ_1)), i.e. $I(t) \geq I^*$ for any $t \in (\tau_0, \tau_1)$. Then we have:*

- (i). $Z(I^*, b) =: Z^*$ is stable under the flow of the equation
- (ii). Let $(v_0, w_0) \in Z^*$, and denote $(v(t), w(t))$ the solution of equations (1) having initial condition (v_0, w_0) at time $t_0 \in [\tau_0, \tau_1]$. Then $t \mapsto v(t)$ is strictly increasing, therefore invertible. Its inverse function $T(v)$ is differentiable, hence so is $W(v) = w(T(v))$, and these variable satisfy the nonlinear differential equation:

$$\begin{cases} \frac{dI}{dv} = \frac{1}{F(v) - W + I(T)} \\ \frac{dW}{dv} = \frac{a(bv - W)}{F(v) - W + I(T)} \end{cases} \quad (2)$$

The explosion time (resp. the value of the adaptation variable at this time) is the limit of $T(v)$ (resp. $W(v)$) when $v \rightarrow \infty$.

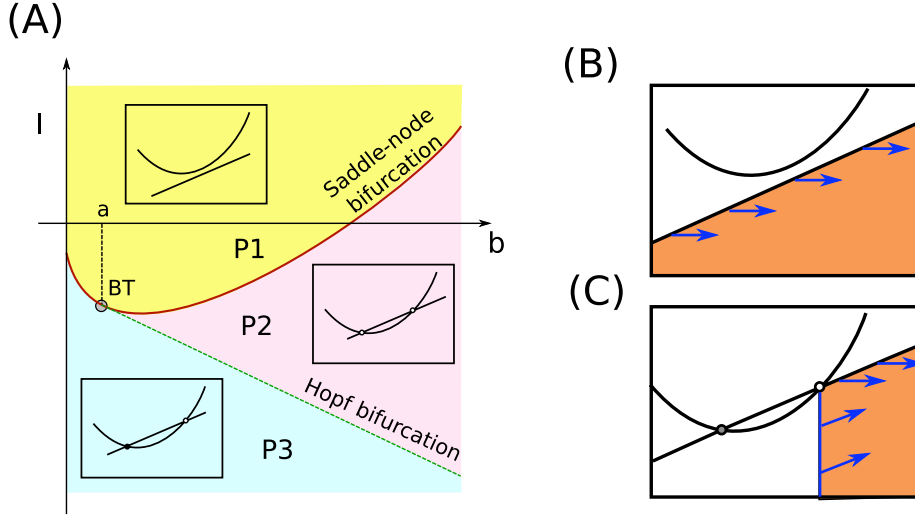


Figure 1: (A) Fixed points and stability in the parameter plane (I, b) . The parameter zone $P1$ corresponds to a case with no fixed points, and the related zone Z is displayed in (B). In the parameter zones $P2$ and $P3$, the Z zone is displayed in (C).

Proof. (i). The stability of $Z^* = Z(I^*, b)$ under the flow of the equation stems from the fact that the vector field points inwards in Z^* on its boundary (see figure 1). Let us first address the case $I^* > -m(b)$. In that case, we have (by definition of $m(b)$) $F(v) - bv + I(t) > 0$ for all $v \in \mathbb{R}$ and all $t \in (\tau_0, \tau_1)$. Z^* is defined as $\{(v, w) ; \Gamma(v, w) < 0\}$ where $\Gamma(v, w) = w - bv$. We use a proof by contradiction. Let us assume that the zone Z^* is not stable under the flow, and that a solution $(v(t), w(t))$ with initial condition $(v_0, w_0) \in Z^*$ at $t_0 \in (\tau_1, \tau_2)$ exits Z^* at time t_1 . This time t_1 is defined as the first exist time of Z^* , i.e.

$$t_1 = \max \{t \geq t_0; (v(t), w(t)) \in Z^*\}.$$

Because of the continuity of the boundary and of the solutions, necessarily we have $w(t_1) = bv(t_1)$. Moreover, at this point we have:

$$\begin{aligned} \left. \frac{d\Gamma(v(t), w(t))}{dt} \right|_{t=t_1} &= a(bv(t) - w(t)) - b(F(v(t)) - w(t) + I(t))|_{t=t_1} \\ &= -b(F(v(t_1)) - bv(t_1) + I(t_1)) \\ &\leq -b(F(v(t_1)) - bv(t_1) + I^*) \end{aligned} \quad (3)$$

This last expression is strictly negative because of the fact that $I^* > -m(b)$. Therefore, since $\gamma : t \mapsto \Gamma(v(t), w(t))$ is a differentiable function of time such that $\gamma(t_1) = 0$ and $\frac{d\gamma}{dt} < 0$, there exists $\eta > 0$ such that $\gamma(t) \leq 0$ on $[t_1, t_1 + \eta)$, which contradicts the maximality of time t_1 .

In the case where $I^* \leq -m(b)$, the zone Z^* is defined by the additional condition that $v > v_+(I^*, b)$. Therefore, on Z^* , we have $(F(v(t_1)) - bv(t_1) + I^*) > 0$. Let us consider $(v(t), w(t))$ a solution with initial condition $(v_0, w_0) \in Z^*$. We have $v_0 > v_+(I^*, b)$. While $(v(t), w(t))$ is in Z^* , $v(t)$ is strictly increasing, and hence the solution will never cross the boundary $v = v_+(I^*, b)$, and can only exit Z^* through the boundary $w = bv$. On this boundary, the same argument as in the case where $I^* > -m(b)$ applies, which ends the proof.

Note that when the current $I(t)$ is constant, this result directly comes from the property that the vector field points inwards the zone Z^* (and inwards any $Z(V)$ for $V > v_+(I, b)$, with the convention $v_+(I, b) = -\infty$ if $I > -m(b)$), making of the zone Z^* a *trapping region* as referred in [22, Chap. 7.3.] (a proof of this property can be found for instance in [28]).

- (ii). Let $(v_0, w_0) \in Z^*$. Then necessarily $(v_0, w_0) \in Z(V)$ for some V such that $v_+(I, b) < V < v_0$. On this zone $Z(V)$, we have $F(v) - w + I \geq F(v) - bv + I \geq \alpha > 0$, therefore $t \mapsto v(t)$ is a strictly increasing function. Moreover, since the derivative of $v(t)$ never vanishes, $t \mapsto v(t)$ is invertible with differentiable inverse function $T(v)$ by application of the inverse function theorem.

By the stability property of Z^* , for all $t \geq 0$ we have $w \leq bv$ and hence

$$\frac{dv(t)}{dt} = F(v) - w + I(t) \geq F(v) - bv + I^*$$

whose solution blows up in finite time under assumption (A1), by the virtue of Gronwall's lemma, see [25].

We denoted $T(v)$ the inverse of the function $t \mapsto v(t)$ was differentiable, and therefore $W(v)$ the composed application $W(v) = w(T(v))$ is also differentiable. We have by definition $v(T(v)) = v$, and differentiating by v we get:

$$\begin{aligned} \frac{dv(T(v))}{dv} &= \frac{dv(t)}{dt} \Big|_{t=T(v)} \frac{dT(v)}{dv} \\ &= (F(v(T(v))) - w(T(v)) + I(T(v))) \frac{dT(v)}{dv} \end{aligned}$$

and it is also equal to one since $v(T(v)) = v$. Therefore we have, since $F(v) - w + I(t)$ never vanishes on $Z(V)$:

$$\frac{dT(v)}{dv} = \frac{1}{F(v) - W(v) + I(T)}$$

and using the differentiation formula of a composed function,

$$\frac{dW}{dv} = \frac{a(bv - W)}{F(v) - W + I(T)}$$

which ends the proof. □

Therefore, as soon as a solution enters the zone Z^* , a spike will be emitted, and both the spike time and the value of the adaptation variable at this time can be computed simulating equation (2). Conversely, any spiking solution will necessarily be contained after some time in the zone Z .

Another property we can deduce from [25] is that the adaptation variable in a left neighborhood of the explosion time is always negligible compared to v , since for F growing faster than $v^{2+\varepsilon}$, w is bounded and v tends to infinity, and for $F(v) \sim v^2$, $W(v)$ grows as a logarithmic function of v . This remark implies that the differential of $w(t)$ tends to infinity at the explosion times of v . However, theorem 1 shows that in the region where the neuron elicits a spike, the time of the spike and the adaptation variable satisfy a well-behaved differential equation (2), fact that will be a cornerstone of our simulation algorithm in section 4.

3 Fixed Time Step Simulation Methods

Most simulation algorithms found in the literature for simulating neuron models of the type of equation (1) involve direct integration of the equations with an fixed time step Euler scheme [10, 4, 26] or a more precise Runge-Kutta scheme. In these simulation algorithms, spikes are emitted when the voltage variable reaches a given threshold θ . The use of such fixed time-step methods for solving this type of blowing-up equations was initially motivated by the observation that the spike time is easily evaluated because of the explosion property of the membrane potential variable v , as discussed in [12], where a typical Euler algorithm is suggested. However, recent research established that in order to accurately simulate these models, one needs to also have an important precision in the evaluation of the adaptation variable at the time of the spike. Indeed, it was shown that this variable governs the spike pattern produced [25, 27], and small changes in the evaluation of this variable can change quantitatively and qualitatively the spike pattern produced.

The crucial question that this observation raises is that beyond the necessary precision in the spike time, the model requires to accurately evaluate the value of the simulated adaptation variable at the time of the spike. In this view, though usual fixed time-step methods might provide a very fair precision to detect the spike time (we will show in the sequel that even this evaluation is subject to discussion and the precision is unbounded as the threshold increases), they are very imprecise for calculating the value of the adaptation variable at the time of the spike as we rigorously show in the present section. This imprecision will substantially modify the value of the time of the next spikes, and this effect will be increasingly important as the number of spikes emitted increases.

We now go into the mathematical details of the precision analysis of such fixed time step methods for simulating the solutions of equation (1). We concentrate on the simpler and most widely used fixed-time step Euler scheme, with

threshold θ and time step τ . The numerical solutions computed through such numerical procedure are solutions of the recursion:

$$\begin{cases} v_{n+1} &= v_n + \tau (F(v_n) - w_n + I(n\tau)) \\ w_{n+1} &= w_n + \tau a (b v_n - w_n) \end{cases} \quad (4)$$

starting from a given initial condition (v_0, w_0) . We denote $X_n := (v_n, w_n)$ and Φ the map such that $X_{n+1} = \Phi(X_n)$ given by the recursion (4).

Lemma 2. *Let us assume that $(v_0, w_0) \in Z^*$ and $\tau a < 1$. Then for all $n \geq 0$, we have $X_n \in Z^*$ and moreover both sequence (v_n) and (w_n) are strictly increasing. Moreover, for all $M > 0$, there exists $n \in \mathbb{N}$ such that $v_n > M$.*

Proof. We reason by induction on n . We know that $X_0 = (v_0, w_0) \in Z^*$. Let us assume that for some $n \geq 0$, we have $X_n = (v_n, w_n) \in Z^*$. Then we have:

$$F(v_n) - w_n + I(n\tau) \geq F(v_n) - b v_n + I^* > 0$$

since $X_n \in Z^*$ in particular implies that $v_n \geq v_+(I^*, b)$. This directly implies that $v_{n+1} > v_n$. Moreover, since in Z^* , we have $w < b v$, it is immediate to show that $w_{n+1} > w_n$, implying that both sequences are increasing.

Moreover, $v_{n+1} > v_n \geq v_0 > v_+(I^*, b)$. Therefore, showing that $X_{n+1} = \Phi(X_n) \in Z^*$ only amounts proving that $w_{n+1} < b v_{n+1}$. We have:

$$\begin{aligned} w_{n+1} - b v_{n+1} &= (w_n - b v_n) + \tau [a (b v_n - w_n) - b (F(v_n) - w_n + I(n\tau))] \\ &= \underbrace{(1 - \tau a)}_{>0} \underbrace{(w_n - b v_n)}_{<0} - \underbrace{b \tau (F(v_n) - w_n + I(n\tau))}_{>0} \\ &< 0. \end{aligned}$$

Eventually, since we have $v_{n+1} - v_n \geq \tau (F(v_n) - b v_n + I^*) > \tau (F(v_0) - b v_0 + I^*) =: K_0$ which is strictly positive constant, we have for all $p \in \mathbb{N}$ the inequality $v_p \geq v_0 + p K_0$, and therefore for all $M > 0$ there exists $n \in \mathbb{N}$ such that $v_n > M$. \square

We therefore observe that for any initial condition in the spiking zone, the Euler simulation scheme will diverge (i.e. $v_n \rightarrow \infty$ when $n \rightarrow \infty$), but does not blow up in finite time, implying in particular that the error made is not a priori bounded if there is no cutoff in the simulation.

As already mentioned, numerical methods consider that the spike time corresponds to the first time the simulated trajectory exceeds a given threshold θ . The thresholded discretization scheme is of order one in τ , meaning that is bounded by a constant depending on the parameters of the model multiplied by τ . Let us now have a closer look to the error made in the thresholded discretized solution. We define the functions $\alpha(\cdot)$ (resp. $\alpha_2(\cdot)$) and $\beta(\cdot)$ (resp. $\beta_2(\cdot)$) corresponding to the first (resp. second) order error in τ of the discretization of v and w as:

$$\begin{cases} v_n = v(n\tau) + \tau \alpha(n\tau) + \tau^2 \alpha_2(n\tau) + O(\tau^3) \\ w_n = w(n\tau) + \tau \beta(n\tau) + \tau^2 \beta_2(n\tau) + O(\tau^3) \end{cases}$$

and let us characterize the functions α and β . We clearly have:

$$\alpha(0) = \alpha_2(0) = \beta(0) = \beta_2(0) = 0$$

Let us now characterize the functions α and β . Following the methods proposed for instance in [7, 9, 20], we have:

$$\begin{aligned} v_{n+1} - v_n &= v(n\tau + \tau) - v(n\tau) + \tau(\alpha(n\tau + \tau) - \alpha(n\tau)) + \tau^2(\alpha_2(n\tau + \tau) - \alpha_2(n\tau)) + O(\tau^3) \\ &= \tau v'(n\tau) + \frac{\tau^2}{2} v''(n\tau) + \tau^2 \alpha'(n\tau) + O(\tau^3) \\ &= \tau (F(v(n\tau)) - w(n\tau) + I(n\tau)) + \frac{\tau^2}{2} v''(n\tau) + \tau^2 \alpha'(n\tau) + O(\tau^3) \end{aligned}$$

and moreover, by the recursion relationship between v_n and v_{n+1} we have:

$$\begin{aligned} v_{n+1} - v_n &= \tau (F(v_n) - w_n + I(n\tau)) \\ &= \tau (F(v(n\tau) + \tau\alpha(n\tau) + O(\tau^2)) - w(n\tau) - \beta(n\tau) + I(n\tau) + O(\tau^2)) \\ &= \tau (F(v(n\tau)) + F'(v(n\tau))\tau\alpha(n\tau) - w(n\tau) - \beta(n\tau) + I(n\tau) + O(\tau^2)) \end{aligned}$$

and therefore, equalizing the two expressions, we get:

$$\alpha'(n\tau) = F'(v(n\tau)) \alpha(n\tau) - \beta(n\tau) - \frac{1}{2} v''(n\tau)$$

proceeding in the exact same fashion for the difference $w_{n+1} - w_n$, we are led to the equations on the first order error of the Euler scheme:

$$\begin{cases} \alpha'(t) &= F'(v(t)) \alpha(t) - \beta(t) - \frac{1}{2} v''(t) \\ \beta'(t) &= a(b\alpha(t) - \beta(t)) - \frac{1}{2} w''(t) \end{cases} \quad (5)$$

Using the equations (1) governing v and w , we obtain the equations:

$$\begin{cases} \alpha' &= F'(v) \alpha - \beta - \frac{1}{2} \left\{ F'(v) (F(v) - w + I) - a(bv - w) + I' \right\} \\ \beta' &= a(b\alpha - \beta) - \frac{a}{2} \left\{ b(F(v) - w + I) - a(bv - w) \right\} \end{cases} \quad (6)$$

It is easy to prove using Gronwall's theorem along the same lines as in [25] that both errors tend to infinity when no threshold is considered, as we also noted from the fact that the continuous solution $v(t)$ blows up in finite time and the discretized version v_n remains finite for all $n \in \mathbb{N}$. We are considering here thresholded equations, and both the simulation algorithm and the continuous time trajectories considered are stopped when the voltage variable reaches a threshold θ , which is considered to be the firing time.

Let us consider a spiking trajectory. From theorem 1 and in lemma 2, we know that as soon as the trajectory enters the spiking zone, the error can be parametrized as a function of the membrane potential $v(t)$. In the sequel, instead of studying the error functions $\alpha(t)$ and $\beta(t)$, it will appear particularly

convenient to study the composed applications $A(v) = (\alpha \circ T)(v) = \alpha(T(v))$ and $B(v) = (\beta \circ T)(v) = \beta(T(v))$ where $T(v)$ is defined in theorem 1 as the inverse of the function $t \mapsto v(t)$ and \circ denotes the composition of applications. These two functions satisfy the equations:

$$\begin{cases} \frac{dA}{dv} = \frac{F'(v)}{F(v)} A - \frac{1}{F(v)} B - \frac{1}{2} \left\{ F'(v) (F(v) - W + I \circ T) - a (bv - W) + I' \circ T \right\} \\ \frac{dB}{dv} = \frac{a}{F(v)} (bA - B) - \frac{a}{2} \left\{ b(F(v) - W + I \circ T) - a (bv - W) \right\} \end{cases}$$

These equations, similarly to initial model's equations, are quite hard to solve, but we can study the behavior close to the threshold (i.e. when v is relatively high) can be approximated by the solution of the equations:

$$\begin{cases} \frac{dA}{dv} = \frac{F'(v)}{F(v)} A - \frac{1}{2} F'(v) \\ \frac{dB}{dv} = \frac{a}{F(v)} (bA - B) - \frac{1}{2} ab \end{cases} \quad (7)$$

These equations can be easily understood heuristically. Indeed, since we know that at the times of the spikes, the membrane potential blows up and the adaptation variable is dominated by the value of the membrane potential variable, the error made on the membrane potential evaluation essentially stems from the divergence membrane potential variable, that asymptotically satisfies an equation of type $\dot{y} = F(y) + I$. This is why the first equation is exactly the same as the one for the error of fixed-time step methods for this one-dimensional equation. The error A computed is the term that mostly disturbs the evaluation of the adaptation variable, and acts on the second equation of (7) as an independent input function. This is coherent with the heuristic argument that the main part of the errors made on the estimation of the adaptation variable at the time of the spike is therefore related to the imprecision in the evaluation of the membrane potential variable.

The study of the first equation of (7) and of the threshold crossing time is quite straightforward at this point. We essentially follow the same steps extending the results to our two-dimensional case. The first equation of (7) is integrated as:

$$A(v) = \frac{1}{2} \left(\log(F(v_0)) - \log(F(v)) \right) F(v)$$

which yields for the error on the adaptation variable:

$$B(v) = -\frac{ab}{2} e^{-\int_{v_0}^v \frac{a}{F(u)} du} \int_{v_0}^v e^{\int_{v_0}^u \frac{a}{F(u_1)} du_1} (\log(F(u)) - \log(F(v_0))) du$$

and the error made on the evaluation of the adaptation variable because of the discretization at the threshold crossing time is therefore equal to $|B(\theta)|$. It is now easy to instantiate the models and find an approximation of the error:

- (i). For $F(v)$ having a polynomial dominant term v^m (which is for instance

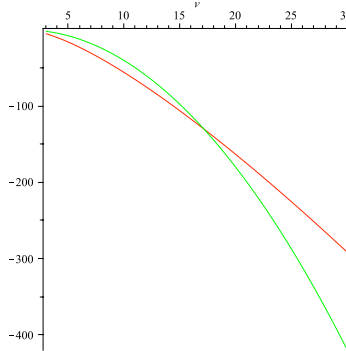


Figure 2: Error made on the estimation of the adaptation variable as a function of the threshold used. We see a fast divergence of the error. Red: quartic case, Green: exponential case

the case of Izhikevich quadratic model and the quartic model), we have:

$$\begin{cases} A(v) &= -\frac{m}{2} v^m \log\left(\frac{v}{v_0}\right) \\ B(v) &= -\frac{a b m}{2} e^{\frac{v-m+1}{m-1} a} \int_{v_0}^v e^{-\frac{u-m+1}{m-1} a} \log\left(\frac{u}{v_0}\right) du \end{cases}$$

- (ii). For $F(v)$ equivalent to an exponential function (as it is the case in the adaptive exponential model), we have the error estimate:

$$\begin{cases} A(v) &= -\frac{1}{2}(v - v_0) e^v \\ B(v) &= -\frac{ab}{2} e^a e^{-v} \int_{v_0}^v e^{-a e^{-u}} (u - v_0) du \end{cases}$$

Both functions are plotted as a function of v in Figure 2, and they are both unbounded and diverging as θ increases. This result implies that the greater the cutoff is the more imprecise the evaluation of the adaptation variable at the cutoff time is imprecise, and that the imprecision diverges as the cutoff value increases. Hence the use of fixed time step methods to approximate such nonlinear integrate-and-fire models leads to substantial errors in the quantitative and qualitative behaviors, as we will further show in section 4.

We now address the following question: is the spike time indeed accurately evaluated by this procedure? The answer to this question was understood to be positive, and the argument given was the divergence of the membrane potential at the time of the spike. However, as we rigorously prove in the sequel, this is not exact. Indeed, the explosion only concerns the differential equation, whereas the numerical procedure does not blow up in finite time, but diverges when time tends to infinity. This induces increasingly large (and even infinite) errors on the

evaluated membrane potential v that produces systematic errors when the spike has a cutoff, errors that diverge when the cutoff tends to infinity. The proof of this fact is quite difficult to produce in the full system. However, as already discussed, because of the fact that during the explosion we have $w = o(v)$, we will restrict the study to the comparison of the recursion $y_{n+1} = y_n + F(y_n)$ and the blowing up solution of $y' = F(y)$, and only for power and exponential F functions, which cover most practical cases.

Let us treat in parallel the power and the exponential cases. Let $m > 1$ be a real number, and consider respectively the ordinary differential equations:

$$\begin{cases} y'_p &= y_p^m \\ y_p(0) &= y_0^p \end{cases} \quad \begin{cases} y'_e &= e^{y_e} \\ y_e(0) &= y_0^e \end{cases}$$

The solution of these ordinary differential equation reads (respectively):

$$\begin{aligned} y_p(t) &= [(y_0^p)^{1-m} - (m-1)t]^{1/(1-m)} \\ y_e(t) &= y_0^e - \log(1 - t e^{y_0^e}) \end{aligned}$$

and blow up at time $t^* = (y_0^p)^{1-m}/(m-1) > 0$ (resp $t^* = e^{-y_0^e}$). The numerical solution from Euler discretization satisfy the recurrence equation:

$$\begin{cases} y_{n+1}^p &= y_n^p + \tau (y_n^p)^m \\ y_{n+1}^e &= y_n^e + \tau e^{y_n^e} \end{cases}$$

with initial condition y_0^p and y_0^e respectively. The approximation error produced by the discretization algorithm was previously computed, and are equal to:

$$\begin{cases} A^p(t) &= -\frac{m}{2} y^p(t)^m \log\left(\frac{y^p(t)}{y_0^p}\right) \\ A^e(t) &= -\frac{1}{2} (y^e(t) - y_0^e) e^{y^e(t)} \end{cases}$$

for $0 \leq t < t^*$, and therefore we have:

$$\begin{cases} y_n^p &= y^p(t) - \tau \frac{m}{2} y^p(t)^m \log\left(\frac{y^p(t)}{y_0^p}\right) + O(\tau^2) \\ y_n^e &= y^e(t) - \tau \frac{1}{2} (y^e(t) - y_0^e) e^{y^e(t)} + O(\tau^2) \end{cases}$$

when $\tau \rightarrow 0$ and for $0 \leq t < t^*$. Let us now define $z^p(k)$ (resp. $z^e(k)$) the continuous variable linear interpolation of y_n^p (resp y_n^e) between two integers n (we have $y^e(n) = z^e(n)$ for all $n \in \mathbb{N}$ and between two consecutive integers the function $k \in [n, n+1] \mapsto z^e(k)$ is linear, and similarly for the polynomial case with indexes p). The relation between $z^p(k\tau)$ and $y^p(t)$ (resp. $z^e(k\tau)$ and $y^e(t)$) is the same as the relation between $y^p(t)$ and y_n^p (resp. $y^e(t)$ and y_n^e) since the errors made by a linear interpolation in an interval of length τ are of order $O(\tau^2)$. Let us now define $n_e^* \in \mathbb{R}$ and $n_p^* \in \mathbb{R}$ such that $z_e(n_e^*) = z_p(n_p^*) = \theta$. We aim at comparing n_e^* and n_e^{**} defined by $y^e(n_e^{**}\tau) = \theta$ (and similarly in the polynomial case). We have:

$$\begin{cases} n_p^{**} &= \frac{(y_0^p)^{1-m}}{(m-1)\tau} - \frac{1}{(m-1)\theta^{m-1}\tau} \\ n_e^{**} &= \frac{1}{\tau} (e^{-y_0^e} - e^{-\theta}) \end{cases}$$

Let now $Z_u = y_u(n^*\tau)$ ($u = e, p$), we have:

$$\begin{cases} \theta &= Z_p - \frac{1}{2}\tau m Z_p^m \log\left(\frac{Z_p}{y_0^p}\right) \\ \theta &= Z_e - \frac{\tau}{2}(Z_e - y_0^e)e^{Z_e} \end{cases}$$

which can be solved up to the second order (by identifying the constant and the linear in τ coefficients of the solution):

$$\begin{cases} Z_p &= \theta + \frac{m\tau}{2} \theta^m \log\left(\frac{\theta}{y_0^p}\right) + O(\tau^2) \\ Z_e &= \theta + \frac{\tau}{2}(\theta - y_0^e)e^\theta + O(\tau^2) \end{cases}$$

and eventually inverting the expression of $y(t)$ one obtains:

$$\begin{cases} n_p^* &= n_p^{**} + \frac{m}{2}\theta^m \log\left(\frac{\theta}{y_0}\right) \\ n_e^* &= n_e^{**} + \frac{1}{2}(\theta - y_0^e) \end{cases}$$

Therefore, there is a constant shift of the estimated spike time produced, that increases as the cutoff increases, and that necessitates small time steps to achieve precision in the spike time chosen.

Therefore, we showed, by analogy to one dimensional ordinary differential equation that capture the explosion of the membrane potential at the time of the spike, that a systematic error is made on the evaluation of the spike time, which is of first order in τ with a bounded coefficient that diverges when the cutoff increases, and most important that the errors made in the estimation of the adaptation variable at the time of the spike, of order one in τ also, have a coefficient that is of large amplitude and that is fast diverging when the cutoff increases. This implies that very small time steps are necessary to achieve a given precision of the simulation, which leads to excessive precision in region of parameters where the vector field is smooth and that questions the efficiency of the obtained simulation algorithm.

We observe that the faster the divergence of the membrane potential, linked with the growth of the function $F(v)$, the larger the error made on the adaptation variable at the cutoff time, and the smaller the error made on the spike time are.

In this section we only dealt with Euler fixed time step methods. However the results still hold for any fixed time step algorithm since these are linked with the very nature of the problem and the explosion at the time of the spike, in addition to the infinite slope of the adaptation variable at the spike time. This issue motivates the introduction of an integration scheme adapted to the nature of the equations we simulate.

4 An Alternative Simulation Algorithm

The explosion, and the infinite slope of the adaptation variable at the time of the spike make the accurate simulation of the spike very delicate as we just

discussed. The simulation algorithm proposed here is based on a simulation of the trajectories in the phase plane. As shown in theorem 1, in the spiking zone, both the time of the spike and the value of the adaptation variable at this time can be accurately and easily computed by solving a smooth ordinary differential equation, given by (2), that governs the trajectory $W(v)$ of the adaptation variable in the phase plane and $T(v)$ the inverse function of $t \mapsto v(t)$. The equations provided are developed in a restricted region of the phase plane denoted Z^* in which one is ensured that the vector field is well-defined at all times. However, it is straightforward to show that this description of the trajectories are valid as long as it does not cross the v -nullcline. The discrete integration scheme makes use of this convenient description of the trajectory in the phase plane in regions of the phase plane where the function $t \mapsto v(t)$ is smoothly invertible, and in the rest of the phase plane close to the v -nullclines, simulates the solutions of the equations (1) with a fixed time step Euler scheme.

Let us assume that we have defined $M > 0$ a real parameter, and the time and space integration steps dt and dv . These three parameters will be used to fix the precision of the algorithm in terms of spike times and value of the adaptation variable at these time in the sequel.

Starting from an initial condition (v_0, w_0) at time t_0 , we build iteratively a sequence (t_n, v_n, w_n) aimed at approximating the variables $(t, v(t), w(t))$ solutions of the continuous ordinary differential equations (1) as follows: given (t_n, v_n, w_n) the numerical solution computed at iteration n , we compute t_{n+1} , v_{n+1} and w_{n+1} as follows:

- (i). If $|F(v_n) - w_n + I(t_n)| < M$, then we define $\tau_n = dt$, and update the values of the triplet as:

$$\begin{cases} v_{n+1} &= v_n + \tau_n (F(v_n) - w_n + I(t_n)) = v_n + dt (F(v_n) - w_n + I(t_n)) \\ w_{n+1} &= w_n + \tau_n a (b v_n - w_n) = w_n + dt a (b v_n - w_n) \\ t_{n+1} &= t_n + \tau_n \end{cases}$$

corresponding to the integration of equation (1) with a constant time step dt . This phase of the integration algorithm is referred as the time-integration phase.

- (ii). if $|F(v_n) - w_n + I(t_n)| > M$, then we define $\tau_n = dv/|F(v_n) - w_n + I(t_n)|$, and update the triplet as:

$$\begin{cases} v_{n+1} &= v_n + \tau_n (F(v_n) - w_n + I(t_n)) = v_n + dv \\ w_{n+1} &= w_n + \tau_n a (b v_n - w_n) = w_n + dv \frac{a (b v_n - w_n)}{F(v_n) - w_n + I(t_n)} \\ t_{n+1} &= t_n + dt = t_n + dv \frac{1}{F(v_n) - w_n + I(t_n)} \end{cases}$$

which corresponds to the integration of (2) with constant v -step dv . This phase of the integration algorithm is referred as the phase-plane integration phase.

Heuristically, this method consists exactly as announced in solving (1) in the regions of the phase plane where the vector field is of small amplitude and solving (2) in the regions of phase plane where the vector field of the dynamical system given by (1) is of large amplitude and yield divergence in finite time of the solutions.

Let us now analyse this algorithm and control the precision of the solution computed. First of all, we analyse the solutions of the algorithm in spiking regions when no threshold is taken into account.

Lemma 3. *For any initial condition (v_0, w_0) in the spiking zone, the simulation of $(t, v(t), w(t))$ presents a voltage variable v that blows up in finite time.*

Proof. Let $(v_0, w_0) \in Z^*$, we have for any n , $(v_n, w_n) \in Z^*$. After a finite number of iterations K , we will have for all $n \geq K$ $F(v_n) - w_n + I(t_n) > M$. Indeed, while $(v_n, w_n) \in Z^*$, lemma 2 implies that v_n is unboundedly increasing and moreover in that zone we have

$$F(v_n) - w_n + I(n\tau) \geq F(v_n) - b v_n + I^*.$$

Since v_n is unboundedly increasing when simulated with Euler scheme, so is $F(v_n) - b v_n + I(n\tau)$ and therefore there exists $K \in \mathbb{N}$ such that $M < F(v_K) - b v_K + I^* \leq F(v_K) - w_K + I(K\tau)$.

The next step v_{K+1}, w_{K+1} is hence computed using the simulation in the phase plane algorithm. Using the same argument as in the proof of lemma 2, we obtain that the sequence (v_n, w_n) stays in a zone where $F(v) - w + I > M$ and $w < b v$, and therefore for all $n \geq K$, the simulation algorithm used is the phase plane algorithm.

We therefore obtain that v_n tends to infinity since $v_{n+1} = v_n + dv$. We now show that the sequence t_n converges to a finite limit. Indeed, we have for all $n \geq K$:

$$\begin{aligned} t_n &= t_K + dv \sum_{k=K+1}^n \frac{1}{F(v_k) - w_k + I(t_k)} \\ &\leq t_K + dv \sum_{k=K+1}^n \frac{1}{F(v_K + (n - K) dv) - b(v_K + (n - K) dv) + I^*}. \end{aligned}$$

The series converges when $n \rightarrow \infty$ because of the hypothesis that F grows faster than $v^{1+\delta}$ for some $\delta > 0$, by a simple sum/integral comparison. \square

In order to compute the precision of the algorithm in the evaluation of the spike time and on the value of the adaptation variable at the time of the spike, we now consider a thresholded version of the simulation algorithm consisting as usual in introducing a cutoff θ . The simulation algorithm is run as long as $v_n < \theta$. When v_n exceeds θ , we instantaneously reset the membrane potential

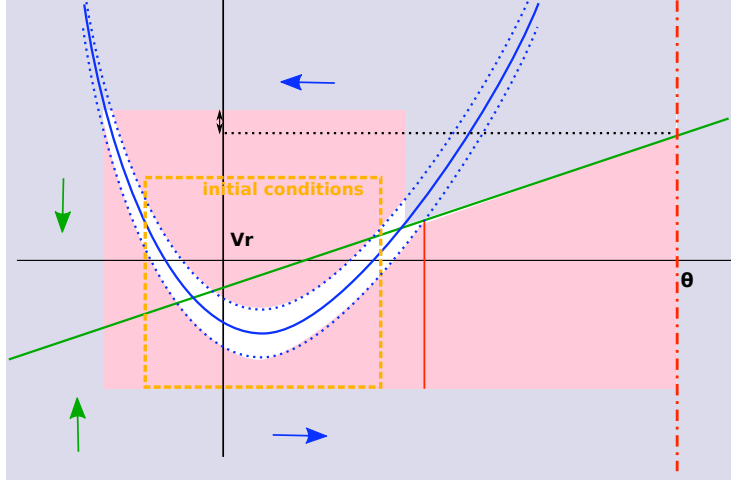


Figure 3: Partition of the phase space. Pink zone: phase-plane integration and white zone: time integration. Orange dotted box: initial conditions.

and update the adaptation variable by defining:

$$\begin{cases} v_{n+1} &= c \\ w_{n+1} &= w_n + d \\ t_{n+1} &= t_n \end{cases}$$

Moreover, the explosion time will indeed be a converging function of the threshold with a precision of order ε , which is an interesting property of the algorithm ensuring that the spike times are accurately estimated, contrasting with the systematic error made by the fixed time-step method, error that diverges when the cutoff value θ tends to infinity. We are now in position to propose a suitable choice of (M, dt, dv) ensuring a fixed precision ε on the adaptation variable at the time of the cutoff $v = \theta$. An optimal choice of (M, dt, dv) would moreover minimize the number of operations necessary to reach the desired precision ε , but this optimal choice is quite difficult to define. To this purpose, let us assume that we consider a bounded set of initial conditions $[v_1, v_M] \times [w_m, w_M]$ (orange box of figure Fig. 3), and let us consider the regions of the phase plane reached by the orbits of the system starting from these initial conditions.

Lemma 4. *For any initial condition $(v_0, w_0) \in [v_m, v_M] \times [w_m, w_M]$, the thresholded trajectories $(v(t), w(t))$ are contained in a compact set $[v_l, \theta] \times [w_d, w_u]$. Moreover, if F grows faster than $v^{2+\delta}$ for some $\delta > 0$, then v_l, w_d and w_u are independent of θ , and the time integration phase takes place in a compact set independent of θ .*

The proof of this quite intuitive lemma is provided in appendix A, and is illustrated in Figure 3: the zones of the phase plane depicted in gray, and the

rest of the phase plane not plotted in the figure constitutes a zones of the phase plane the orbit starting from any initial condition in the subset defined will never reach.

Now that we restricted possible initial conditions of the system, we know from lemma 4 that the values of (v, w) on the orbits are contained in a bounded set. For the quadratic model, these values depend on the cutoff value θ since the adaptation variable at the times of the spike diverges, and for models satisfying assumption (A2), it can be defined independently of θ . On this bounded set, the functions $F(v) - w + I$ and $a(bv - w)$ are both bounded, differentiable with bounded derivatives, which allows definition of time steps dt and phase-space step dv that uniformly ensure a given precision of the numerical algorithm. This fact is discussed in appendix A.

A more efficient method that minimizes the computation operations consists rather in choosing varying steps depending on the values of the variables, such that these integration steps ensure exactly a precision bounded by ε at each integration time.

- (i). The numerical time integration consists of an Euler scheme approximating the solutions of the equations (1). The second derivative of $v(t)$ and $w(t)$ read:

$$\begin{cases} v''(t) = F'(v)(F(v) - w + I) - a(bv - w) + I'(t) \\ w''(t) = a(b(F(v) - w + I)) - a(bv - w) \end{cases}$$

where x' denotes the derivative of $x(t)$ with respect to time. The larger time step dt ensuring a precision of order ε at the point (v, w) therefore reads:

$$\tilde{dt}(v, w) = \frac{\varepsilon}{\max(|v''(t)|, |w''(t)|)}$$

This varying time step allows achieving the desired precision in a minimal number of operations.

- (ii). The numerical phase space integration consists of an Euler scheme approximating the solutions of the equations (2) on a compact subset of the phase space. The second derivative of $T(v)$ and $W(v)$ with respect to v (denoted with a double dot) reads:

$$\begin{cases} \ddot{W}(v) = \frac{ab}{F(v) - W + I} - \frac{a(bv - W)}{(F(v) - W + I)^2} - \frac{aF'(v)(bv - W)}{(F(v) - W + I)^2} \\ \quad - \frac{a(bv - W)(a(bv - W) + I'(T))}{(F(v) - W + I)^3} \\ \ddot{T}(v) = -\frac{(F(v) - W + I)^3}{F'(v)(F(v) - W + I) - a(bv - W) + I'(T)} \end{cases}$$

With these expressions, we are in position to choose an optimal integration step depending on the values of the variables (v, w) ensuring the desired precision:

$$\tilde{dv}(v, w) = \frac{\varepsilon}{\max(|\ddot{W}(v)|, |\ddot{T}(v)|)}.$$

In appendix A, we show that these integration steps can be chosen uniformly for all (v, w) as long as we only consider initial conditions contained in a bounded subset of the phase space.

Note that the choice of the value of M impacts the number of operations performed. Choosing a large value for M implies that the time integration phase is emphasized, whereas a small value of M emphasizes the phase space integration.

This algorithm can therefore be seen as a varying time-step integration method, and the phase-plane interpretation allows to derive the precision of the algorithm. These calculations also provide a simple criterion to choose the optimal dt and dv in each phase to ensure a precision of order ε in both the explosion time and the value of the adaptation variable at this time in a minimal number of operations.

Note that in our simulation algorithm, we also add a control on the value of the integration step in order for these not to be too large in regions where the vector field varies slowly and choose a maximal value of the integration steps. This varying integration step method is our method of choice in the examples and in the results.

Discussion

In this paper we studied the error produced by fixed time step integration methods for nonlinear bidimensional neuron models and showed that the error produced, even if these are of order 1 in the time step chosen, are proportional to a function of the parameters and of the cutoff chosen to identify the spikes, and this function is unbounded as the threshold increases. This fact implies that in order to achieve a fixed precision on the global algorithm and accurately simulate the explosion time, one needs to use a large enough threshold value θ and a very small time step in order to accurately estimate the spike time and the value of the adaptation variable at this time. We saw that the main difficulty arises close from the spike time, since the explosion of the membrane potential variable produces large errors and the differential of the adaptation variable also diverges at this time. The small time step needed to accurately evaluate the crucial values of the spike time and the adaptation variable at these time will result in an excessive precision in regions where the vector field is smooth and an increased computational time.

In Figure 2, we plotted the error made on the evaluation of the adaptation variable as a function of the cutoff θ chosen. Let us denote by $E(\theta)$ such a function. The error is then proportional to $E(\theta) dt$ and therefore these curves are directly related to the time step needed to achieve a given precision. If one wants to get a bounded by ε on the adaptation variable, one therefore needs to choose $dt = \varepsilon/|E(\theta)|$ which implies that the number of operations needed is proportional to $|E(\theta)|/\varepsilon$, which diverges as the threshold increases.

In order to overcome this difficulty, we proposed an alternative algorithm that is based on the numerical computation of the orbits in the phase plane in

regions where the modulus of the vector field is large enough. This algorithm, similar to classical variable integration step methods, allows to choose optimal steps in order to achieve the desired precision in a minimal number of operations, which can be uniformly bounded as shown in section 4. Therefore this method provides us with a stable method that allows considering large thresholds and that precisely evaluates the spike times and the value of the adaptation variable at these times in a reduced number of operations.

We now discuss the importance of numerical errors on the simulations from a computational neuroscience viewpoint. The models we addressed in this paper are particularly used to simulate spike times in order to identify different spike patterns, such as regular spiking, bursting and chaotic spiking (see e.g. [10, 12, 2, 24, 27]). We showed that the spike times and the adaptation variable at these times can be substantially modified when using fixed time step methods, and this effect can produce qualitative distinctions between firing patterns. Indeed, it was shown in [27] that the spike pattern depended sensitively on the value of the adaptation variable at the times of the spikes and that these spike patterns undergo bifurcations. Since we have seen that fixed time-step Euler scheme produces a systematic negative error (i.e. the evaluated spike time was strictly inferior its actual value as a solution of the continuous differential equations), this error can make the system cross bifurcation points and change spike patterns. We illustrate this fact for instance on the quadratic model with original parameters provided in [10]: in this case, $F(x) = 0.04x^2 + 5x + 140$ and $c = -59.9$, parameters that were chosen to fit intracellular recordings. By choosing the parameters $a = 0.02$, $b = 0.19$, $d = 1.15$, $\theta = 30$ and a constant input $I = 7.6$, the system produces bursts with two spikes per bursts. We simulate for $T = 0$ to 1000 in order to record a long enough spike train, and plot the sequence of values of the adaptation variable at the time of the spikes. These values allow discriminating between bursts (that produce periodic sequences) and regular spiking (that correspond to a fixed point of the sequence). We observe that for $dt < 0.05$ the bursting nature of the trajectory is recovered, but for any time step greater than this value, the spike pattern produced appears as a regular spiking behavior. Therefore, on our simulation interval, one needs to perform at least 20 000 operations to obtain the desired spike train, and at this resolution the burst is quite perturbed by numerical imprecision. For the same parameters, since we observe that the numerical values of the adaptation variable at the time of the spike are separated by 0.33, the desired precision to ensure that we distinguish the two points is at least 0.15. We choose $\varepsilon = 0.1$ and compute the trajectory. This precision being fixed, the algorithm performs 2000 operations and achieves a great precision on the value of the adaptation variable at the spike time, that is not comparable to what is obtained by the fixed time-step Euler method. Actually the precision of the algorithm is smaller than the value chosen because of the control put on the value of the integration steps in order for these not to exceed certain values in regions where the vector field varies slowly. For such precision, one would necessitate to use $dt = 0.01$ corresponding actually to 100 000 operations. Therefore, the computational gain of using the new algorithm instead of a fixed time step Euler method ranges

from 10 to 50.

In models satisfying assumption (A2) such as the quartic and the exponential adaptive models, the adaptation variable at the times of the spike converges, and therefore it can be very convenient to use large values of the cutoff in order to get rid of the artificial strictly voltage threshold similar to classical integrate-and-fire models [16, 21] by a more realistic spike initiation (see e.g. [17, 5]) and fully taking advantage of this property of nonlinear integrate-and-fire neurons. The algorithm proposed here allows considering larger values of cutoff θ without a prohibitive increasing the computational time, which allows more accurately simulating the blowing-up system.

The algorithm we proposed here can easily be used for simulations of networks composed of neurons of the type studied here. This new method will therefore be very useful for the simulations of very large networks using such models by providing a more precise and computationally more efficient method to simulate the solutions of these equations.

Acknowledgement This work was partially supported by ERC grant NERVI-227747

A Trajectories starting from a given set of initial conditions are bounded

In this appendix we demonstrate lemma 4, which is recalled here:

Lemma 5. *For any initial condition $(v_0, w_0) \in [v_m, v_M] \times [w_m, w_M]$, the thresholded trajectories $(v(t), w(t))$ are contained in a compact set $[v_l, \theta] \times [w_d, w_u]$. Moreover, if F grows faster than $v^{2+\delta}$ for some $\delta > 0$, then v_l , w_d and w_u are independent of θ , and the time integration phase takes place in a compact set independent of θ (see Figure 3: the zones of the phase plane depicted in gray, and the rest of the phase plane not plotted in the figure constitutes a zones of the phase plane the orbit starting from any initial condition in the subset defined will never reach).*

Proof. Let $(v_0, w_0) \in [v_m, v_M] \times [w_m, w_M]$ and consider the orbit of the dynamical system (1) with (v_0, w_0) an initial condition in this region. We start by considering $I(t)$ constant. The trajectories for $I(t)$ non constant will be bounded by the values the orbit can reach for the vector associated with the minimal and maximal values of the $I(t)$ because of the monotony of the vector field and because of Gronwall's inequality.

First of all, the case where $F(v) - bv + I > 0$ for all v corresponding to the case where the nullclines never intersect is simple to treat. Indeed, in that case the spiking zone is simply $\{(v, w); w \leq bv\}$ and it is a trapping zone, i.e. any trajectory with initial condition in the spiking zone will never escape from it. For any initial condition in this spiking zone (zone I in Figure 3(A)), $w_0 \leq w(t) \leq bv(t)$ and $v_0 \leq v(t) \leq \theta$ and hence $w(t) \in [w_m, \max(b\theta, w_M)]$ and

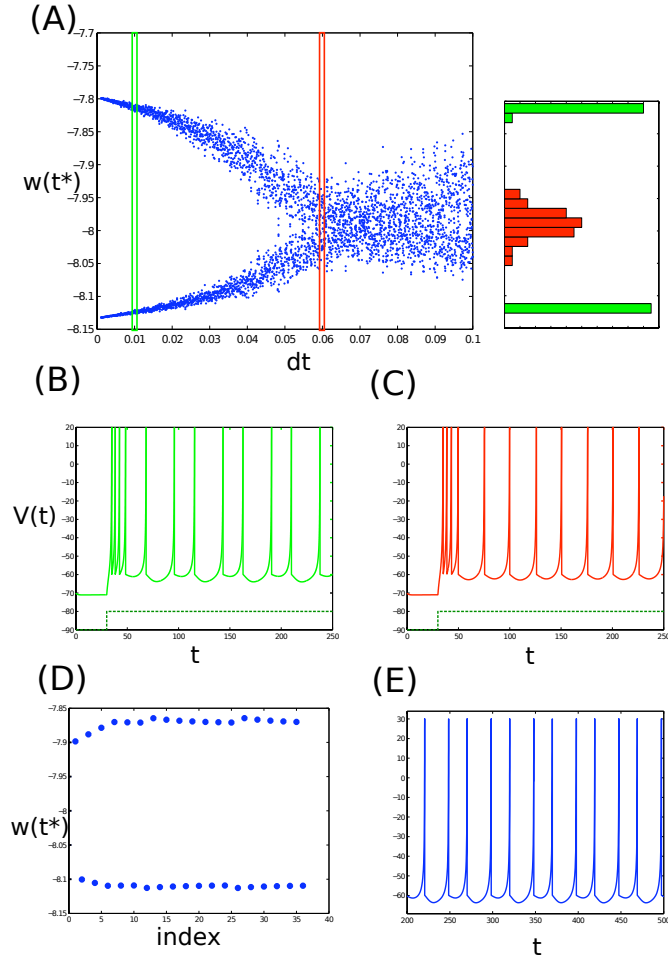


Figure 4: Simulation of the quadratic model with parameters given in the text. (A) represents the value of the adaptation variable at the spike times as a function of a fixed time-step dt for an Euler scheme. (left) We observe that the bursting nature of the trajectory is lost and one recovers a regular spiking behavior if the time step is not small enough. (right) represents the histogram of these values for $dt = 0.01$ (green) and $dt = 0.1$ (red). (B) and (C) correspond to sample trajectories computed for $dt = 0.01$ and $dt = 0.1$ respectively (stopped at $t = 250$ for legibility). (D) represents the sequence of reset values for the variable integration step algorithm with precision set at $\varepsilon = 0.1$ (similar to (A) but for a fixed integration scheme and where the abscissa corresponds to the number of spike fired before this value is obtained) and (E) a sample trajectory simulated by this algorithm.

$v \in [v_m, \theta]$. If (v_0, w_0) in zone II of Figure 3(A), i.e. if $bv_0 \leq w_0 \leq F(v_0) + I$, the variable $v(t)$ is increasing all along the trajectory and therefore $\theta \geq v(t) \geq v_0 \geq v_m$. The variable $w(t)$ is initially decreasing (therefore bounded by $w_0 \leq w_M$) before reaching the w -nullcline and then increases in the spiking zone and where trajectories are bounded by $b\theta$. Hence $bv_m \leq bv_0 \leq w(t) \leq \max(w_M, b\theta)$. Eventually in zone III of Figure 3(A), i.e. $w_0 \geq F(v_0) + I$, both the value of $v(t)$ and of $w(t)$ are initially decreasing and will reach in finite time the v -nullcline where it enters zone II. Before reaching this zone, the minimal value reached by the variable $v(t)$ is greater than $v_1 = \min(F^{-1}(w_0 - I))$ and smaller than $v_0 \leq v_M$, and the value of $w(t)$ is smaller than $w_0 \leq w_M$ and greater than $\min(F(v) + I)$ which is reached at a point denoted v^* . From these initial conditions in zone II the same analysis as previously done extends the boundaries to $\theta \geq v(t) \geq \min(v_m, v_1)$ and $b \min(v_1, v_m, v^*) \leq w(t) \leq \max(w_M, b\theta)$.

After resetting, the initial condition is on the line c with values of w in the interval $[\min(v_1, v_m, v^*) + d, \max(w_M, b\theta) + d]$ and a similar analysis provides us with the boundaries

$$(v(t), w(t)) \in [\min(v_m, v_1^*)] \times [b \min(v_1^*, v_m, v^*, c), \max(w_M, b\theta)]$$

with $v_1^* = \min(F^{-1}(\max(w_M, b\theta) + d - I))$.

Moreover, in the case where F grows faster than $v^{2+\delta}$ for some $\delta > 0$, it was proved in [27] by a thorough analysis of the spike and reset process that the maximal value reached by the variable w in the spiking zone is bounded by a value Φ^* independently of the cutoff, making the boundaries provided independent of θ .

In the case where the nullclines do meet, we perform a similar analysis. First of all, it is clear that the value of $w(t)$ before resetting is bounded by $\max(w_M, b\theta)$. After the reset, w is therefore upperbounded by $w_u = \max(w_M, b\theta) + d$. The value of v is cut at θ and hence any thresholded trajectory have $v(t) \leq \theta$. We assume that $F(c) - w_u + I^* < 0$. At this point we therefore have v decreasing, and the minimal value of v after a reset corresponds to this value and is lowerbounded by the solution of $F(v) - w_u + I^* = 0$ i.e. $v \geq \min(F^{-1}(w_u - I^*))$. If $w_u < F(c) + I^*$, then the value of v on any reseted trajectory is greater than c . Therefore, we conclude that $v \geq v_l = \min(c, v_m, \min(F^{-1}(w_u - I^*)))$. Eventually, this value provides us with a minimal value of w along the trajectories. Indeed, the minimal value of v after reset implies that any reseted trajectory will have $w(t) \geq bv_l$. If w_0 is such that $F(v_0) - w_0 + I^* < 0$, then in this region

First of all, because of the structure of the flow and the reset condition, the maximal value reached on the reset line $v = c$ is upperbounded by $b\theta + d$. This bound can be made independent of θ if the function F grows faster than $v^{2+\delta}$ for some $\delta > 0$. In that case, there exists a value denoted $\Phi^* + d$, as defined in [27], and corresponding to the value where the adaptation variable will be reset when starting just below $w^* = F(c) + I^*$. This value does not depends on θ and can be evaluated previously before simulations, by simulating equation (2) with initial condition (c, w_0) with w_0 slightly below $w^* = m(b)$ the minimum of the function $F(v) - bv + I$. Note that if θ is not chosen very large, or if one

does not want to vary θ , this value $\Phi(w^*)$ can be for instance replaced by the an upper-bound $b\theta + d$ (choice depicted in the figure). Therefore the values of the adaptation variable at the time of the spike have the global upper-bound $w_u = \max(v_M, \Phi(w^*) + d)$ or $w_u = \max(v_M, b\theta + d)$. This maximal value defines a left boundary of the values of v . Indeed, denoting $v_1 = \min\{v, F(v) - w_u + I^* = 0\}$ (there are two possible values of v_1 because of the convexity of F), we have $v \geq v_l := \min(v_1, v_m)$. This value in turn allows defining the lower w value trajectories can have. As soon as the w -nullcline is crossed, w increases. Therefore, w is larger than $w_l := \min(bv_l, w_m)$. It has a typical structure as depicted in figure Fig. 3. The set where the algorithm (i) is used is the white space in figure 3, and is strictly included in $[v_l, v_+(I^* - \varepsilon, b)] \times [w_l, w_u]$. \square

Now that we restricted possible initial conditions of the system, we know from lemma 4 that the values of (v, w) on the orbits are contained in a bounded set. For the quadratic model, these values depend on the cutoff value θ since the adaptation variable at the times of the spike diverges, and for models satisfying assumption (A2), it can be defined independently of θ . On this bounded set, the functions $F(v) - w + I$ and $a(bv - w)$ are both bounded, differentiable with bounded derivatives, which allows definition of time steps dt and phase-space step dv that uniformly ensure a given precision of the numerical algorithm.

Indeed, in both the time integration stage and the phase space integration stage, the integration method is an Euler scheme, either integrated in time or in the v variable. In these cases, it is well known that the precision of the method is bounded by the second derivative of the integrated variables multiplied by the integration step (the proof of this fact is close from the analysis performed in section 3). More specifically, we have:

- (i). The numerical time integration consists of an Euler scheme approximating the solutions of the equations (1) on a compact subset of the phase space where $|F(v) - w + I| \leq M$. Moreover, the values of the variable (v, w) are contained in a compact set that can be chosen independent of the value of θ under assumption (A2) as already discussed. The second derivative of $v(t)$ and $w(t)$ read:

$$\begin{cases} v''(t) = F'(v)(F(v) - w + I) - a(bv - w) + I'(t) \\ w''(t) = a(b(F(v) - w + I)) - a(bv - w) \end{cases}$$

where x' denotes the derivative of $x(t)$ with respect to time. We also note that the time-integration is performed on an even more reduced zone of the phase space. Indeed, the fact that $|F(v) - w + I| < M$ implies that $F(v) \leq M + w_u - I^*$ defining an interval of values of v where the integration is performed and on this compact set, we clearly have $C_1 > 0$ and $C_2 > 0$ such that $|a(bv - w)| < C_1$ and $|F'(v)| < C_2$. Therefore choosing $dt < \varepsilon / (\max(C_2M + C_1 + \|I'\|_\infty, |ab|M + C_2))$, we are ensured to have a precision of the order ε on the evaluated value of $v(t)$ and $w(t)$. Moreover, besides the uniform bound on the error that allows choosing

a time-step dt ensuring a precision of order ε at any point of the phase plane where the time integration is performed, the analysis allows defining an optimal time step dt depending on the point (v, w) and ensuring the desired precision:

$$\widetilde{dt}(v, w) = \frac{\varepsilon}{\max(|v''(t)|, |w''(t)|)}$$

This varying time step allows achieving the desired precision in a minimal number of operations.

- (ii). The numerical phase space integration consists of an Euler scheme approximating the solutions of the equations (2) on a compact subset of the phase space. The second derivative of $T(v)$ and $W(v)$ with respect to v (denoted with a double dot) reads:

$$\begin{cases} \ddot{W}(v) = \frac{ab}{F(v) - W + I} - \frac{a(bv - W)}{(F(v) - W + I)^2} - \frac{aF'(v)(bv - W)}{(F(v) - W + I)^2} \\ \quad - \frac{a(bv - W)(a(bv - W) + I'(T))}{(F(v) - W + I)^3} \\ \ddot{T}(v) = -\frac{F'(v)(F(v) - W + I) - a(bv - W) + I'(T)}{(F(v) - W + I)^3} \end{cases}$$

and here again, we can find $C_3 > 0$ and $C_4 > 0$ such that: $|a(bv - W)| \leq C_3|F(v) - W + I|$ and $|F'(v)| \leq C_4|F(v) - W + I|$ and if we defining dv such that:

$$dv \max \left(C_3 C_4 + \frac{|ab| + C_3 + C_3^2}{M} + \frac{\|I'\|_\infty C_3}{M^2}, \frac{C_4}{M} + \frac{C_3}{M^2} + \frac{\|I'\|_\infty}{M^3} \right) \leq \varepsilon$$

we ensure that the error on $W(v)$ and $T(v)$ bounded by ε . Here again, we are in position to choose an optimal integration step depending on the values of the variables (v, w) ensuring the desired precision:

$$\widetilde{dv}(v, w) = \frac{\varepsilon}{\max(|\ddot{W}(v)|, |\ddot{T}(v)|)}.$$

The evaluation of the values of C_1, C_2, C_3, C_4 is quite difficult in the most general case. However, as mentioned, we can choose a varying integration steps \widetilde{dt} and \widetilde{dv} depending on the values of the variables that ensures exactly a precision bounded by ε at each integration time, as done in the main text.

It is interesting to note that the choice of M impacts the values of dt and dv and therefore the number of operations necessary to integrate the system for a fixed precision ε . The larger M is chosen, the smaller dt is and the larger dv is, meaning that we emphasize the time integration (phase (i) of the algorithm) and give less importance to the phase space simulation (phase (ii) of the algorithm). Conversely, if M is small, the resulting dv will be smaller and dt larger, and the scheme will emphasize the phase-space integration. A balanced choice of M will allow an optimal simulation of the model by taking advantage of both integration methods, in the sense that it will perform the smaller number of operations for a given precision ε .

References

- [1] Laurent Badel, Sandrine Lefort, Romain Brette, Carl C. H. Petersen, Wulfram Gerstner, and Magnus J. E. Richardson. Dynamic i-v curves are reliable predictors of naturalistic pyramidal-neuron voltage traces. *Journal of Neurophysiology*, 99:656–66, feb 2008. PMID: 18057107 doi: 01107.2007.
- [2] R. Brette and W. Gerstner. Adaptive exponential integrate-and-fire model as an effective description of neuronal activity. *Journal of Neurophysiology*, 94:3637–3642, 2005.
- [3] C. Clopath, R. Jolivet, A. Rauch, H.R. Lüscher, and W. Gerstner. Predicting neuronal activity with simple models of the threshold type: Adaptive Exponential Integrate-and-Fire model with two compartments. *Neurocomputing*, 70(10-12):1668–1673, 2007.
- [4] Claudia Clopath, Lorric Ziegler, Eleni Vasilaki, Lars Busing, and Wulfram Gerstner. Tag-trigger-consolidation: a model of early and late long-term potentiation and depression. *PLoS Comput Biol*, 4(12):e1000248, Dec 2008.
- [5] N. Fourcaud-Trocme, D. Hansel, C. van Vreeswijk, and N. Brunel. How Spike Generation Mechanisms Determine the Neuronal Response to Fluctuating Inputs. *Journal of Neuroscience*, 23(37):11628, 2003.
- [6] W. Gerstner and W. Kistler. *Spiking Neuron Models*. Cambridge University Press, 2002.
- [7] E. Hairer and C. Lubich. Asymptotic expansions of the global error of fixed-stepsize methods. *Numerische Mathematik*, 45(3):345–360, 1984.
- [8] B. Hille. *Ion channels of excitable membranes*. Sinauer Sunderland, Mass, 2001.
- [9] E. Isaacson and H.B Keller. *Analysis of numerical methods*. John Wiley & Sons, New York, 1994.
- [10] E. Izhikevich. Simple model of spiking neurons. *IEEE Transactions on Neural Networks*, 14(6):1569–1572, 2003.
- [11] E.M. Izhikevich. Which model to use for cortical spiking neurons? *IEEE Trans Neural Netw*, 15(5):1063–1070, September 2004.
- [12] E.M. Izhikevich. *Dynamical Systems in Neuroscience: The Geometry of Excitability And Bursting*. MIT Press, 2007.
- [13] Eugene M Izhikevich and Gerald M Edelman. Large-scale model of mammalian thalamocortical systems. *Proc Natl Acad Sci U S A*, 105(9):3593–3598, Mar 2008.

- [14] R. Jolivet, R. Kobayashi, A. Rauch, R. Naud, S. Shinomoto, and W. Gerstner. A benchmark test for a quantitative assessment of simple neuron models. *Journal of Neuroscience Methods*, 169(2):417–424, 2008.
- [15] Renaud Jolivet, Felix Schurmann, Thomas K Berger, Richard Naud, Wulfram Gerstner, and Arnd Roth. The quantitative single-neuron modeling competition. *Biol Cybern*, 99(4-5):417–426, Nov 2008.
- [16] L Lapique. Recherches quantitatives sur l’excitation des nerfs traitée comme une polarisation. *J. Physiol. Paris*, 9:620–635, 1907.
- [17] P.E. Latham, B.J. Richmond, P.G. Nelson, and S. Nirenberg. Intrinsic dynamics in neuronal networks. I. Theory. *J. Neurophysiol.*, 83:828–835, 2000.
- [18] H. Markram, M. Toledo-Rodriguez, Y. Wang, A. Gupta, G. Silberberg, and C. Wu. Interneurons of the neocortical inhibitory system. *Nature Reviews Neuroscience*, 5:793–804, 2004.
- [19] R Naud, N Macille, C Clopath, and W Gerstner. Firing patterns in the adaptive exponential integrate-and-fire model. *Biological Cybernetics*, 99(4–5):335–347, nov 2008.
- [20] J.M. Sanz-Serna and J.G. Verwer. A study of the recursion $y_{n+1} = y_n + Ty_n^m$. *Journal of Mathematical Analysis and Applications*, 116:456–464, 1986.
- [21] R. B. Stein. Some models of neuronal variability. *Biophysical Journal*, 7:37–68, 1967.
- [22] S.H. Strogatz. *Nonlinear dynamics and chaos*. Addison-Wesley Reading, MA, 1994.
- [23] J. Touboul. *Nonlinear and stochastic models in neuroscience*. PhD thesis, Ecole Polytechnique, dec 2008.
- [24] Jonathan Touboul. Bifurcation analysis of a general class of nonlinear integrate-and-fire neurons. *SIAM Journal on Applied Mathematics*, 68(4):1045–1079, 2008.
- [25] Jonathan Touboul. Importance of the cutoff value in the quadratic adaptive integrate-and-fire model. *Neural Computation*, 21(8):2114–2122, 2009.
- [26] Jonathan Touboul and Romain Brette. Dynamics and bifurcations of the adaptive exponential integrate-and-fire model. *Biological Cybernetics*, 99(4–5):319–334, nov 2008. PMID: 19011921 DOI: 10.1007/s00422-008-0267-4.
- [27] Jonathan Touboul and Romain Brette. Spiking dynamics of bidimensional integrate-and-fire neurons. *SIAM Journal on Applied Dynamical Systems*, 8(1462-1506), 2009.

- [28] Claude Viterbo. Systèmes dynamiques et équations différentielles. Lecture Notes of the École Polytechnique, 2005.